Miniaturized metabolomics methods for enabling the study of biomass-restricted samples

He, B.

Chapter IV

A micro-flow liquid chromatography-mass spectrometry method for the quantification of oxylipins in volume-limited human plasma

Based on:

Bingshu He, Rawi Ramautar, Marian Beekman, P. Eline Slagboom, Amy Harms, Thomas Hankemeier

A micro-flow liquid chromatography-mass spectrometry method for the quantification of oxylipins in volume-limited human plasma

ELECTROPHORESIS 2025; DOI: 10.1002/elps.202400151

Abstract

Oxylipins are well-known lipid mediators in various inflammatory conditions. Their endogenous concentrations range from low picomolar to nanomolar and there are growing demands to determine their concentrations in low volume matrices for pathological studies, including blood, cerebrospinal fluids from animal disease models, infants, and microsampling devices. Most of the published quantification methods for comprehensive profiling of oxylipins still require more than 50 µL plasma as a starting volume to detect these low levels. The aim of our study is to develop a sensitive and reliable method for the quantification of oxylipins in volume-limited human plasma samples. We established and validated a micro-LC-MS/MS method that requires only 5 µL of human plasma for the determination of 66 oxylipins. The optimized micro-LC-MS/MS method utilized a flow rate of 4 µL/min with a 0.3-mm inner diameter column. With an injection volume of 3 µL, our method provides limits of detection in the range from 0.1 pM to 91.9 pM, and limits of quantification ranging from 0.3 pM to 306.2 pM. The sensitivity enhancement compared to conventional flow ranged from 1.4 to 180.7 times for 51 compounds depending on their physical-chemical properties. After validation, the method was applied to analyze 40 plasma samples from a healthy aging study to demonstrate robustness and sensitivity.

1. Introduction

Oxylipins are a group of signaling lipids derived from polyunsaturated fatty acids (PUFAs) through enzymatic or non-enzymatic oxidation processes. Non-esterified or free oxylipins function as important lipid mediators in multiple physiological processes as well as disease pathologies. Cardiovascular diseases, obesity, type II diabetes, and neurological disorders have been linked to abnormal oxylipin signaling [1, 2]. Oxylipins include some well-studied subclasses such as prostaglandins (PGs), arachidonic acid (AA) derived isoprostanes, AA and eicosapentaenoic acid (EPA) derived prostanoids, AA derived leukotrienes, and lipoxins, which are involved in inflammation, blood clotting, immune response, cardiovascular diseases, and tumor progression [3-7].

As the most direct and easy to sample matrix, plasma is commonly utilized for studying the onset and progression of pathological processes. Despite the increasing demand for oxylipin profiling and understanding their functions, currently available LC-MS methods for the quantification of PUFAs and their derivatives often fall short when dealing with volume-limited plasma samples [8-11]. Although plasma from adults is not normally recognized as volume-limited, when one sample set has to be aliquoted to multiple analytical platforms for a comprehensive multi-omics analysis, only a limited volume is available for each platform. On the other hand, the sampling techniques in healthcare favour sampling low volumes (below 10 µL) to ease the pain for patients [12, 13] and improve wellness of experimental animals [14]. The issue of volume mismatch between sampling and sample analysis can be addressed by employing a miniaturized LC-MS workflow, which allows high detection sensitivity with a minimal sample volume.

One example of how a miniaturized workflow can increase sensitivity was presented by Cebo et al. [15] who established a micro-LC-MS/MS method for accurate quantification of 42 oxylipins in plasma using a flow rate of 30 µL/min. Although the method allowed for the quantitation of some oxylipins down to the picogram level, a relatively large volume of plasma (500 µL) was used, and the sample was up-concentrated to 100 µL to achieve the required detection limits. A further down-scaling in flow rate may lead to higher sensitivity which enables the quantification of oxylipins using less starting material.

In this study, we established a micro-LC-MS workflow for the quantification of 66 oxylipins in 5 µL human plasma. Selected reaction monitoring (SRM) was applied in a targeted method in negative ion mode. Multiple electrospray ionization sources were compared, corona discharge was minimized, and analytical performance was optimized. A reverse phase C18 column with a 0.3-mm inner diameter was used for this method at a flow rate of 4 µL/min. The method underwent validation following the bioanalytical method validation guidelines from EMA (2009). The sensitivity enhancement was evaluated by comparing the limits of detection and limits of quantification with a published conventional flow UHPLC-MS method [16]. The validated method was applied to 40 human plasma samples from a healthy aging study with 5-µL as starting volume. 28 oxylipins were quantified from picomolar to nanomolar level. This underscores its potential value for future studies that demand high sensitivity in determining oxylipin concentrations in volume-limited samples.

2. Material and methods

2.1 Chemicals and materials

Ultra-performance liquid chromatography grade acetonitrile (ACN) and methanol (MeOH) were purchased from Biosolve (Valkenswaard, Netherlands). 1-Butanol (BuOH) was acquired from Boom (Meppel, Netherlands). Methyl tert-butyl ether (MTBE), acetic acid (100%, LC-MS grade), butylated hydroxytoluene (BHT), ethylenediaminetetraacetic acid (EDTA) were from SigmaAldrich (Zwijndrecht, Netherlands). Citric acid monohydrate and disodium hydrogen phosphate were obtained from Merck (Darmstadt, Germany). Purified water was obtained from a Milli-Q PF Plus system (Merck Millipore, Burlington, Massachusetts, United States). Standards and deuterated standards for oxylipins were purchased from Cayman Chemicals (Ann Arbor, Michigan, United States). The purchasing information and abbreviations of all the targeted oxylipins and labeled standards are listed in **Supplementary Table 1**.

2.2 Preparation of standards solutions and calibrant solutions

Stock solutions of oxylipins and labeled standards were dissolved in MeOH containing BHT (0.4 mg/mL) to 1 mg/mL. The oxylipins standard stock solutions were diluted to 11

calibrant points (C1 to C11) subsequently. Internal standards (ISTD) were spiked in each calibrant point and sample to reach a final concentration of 20 nM. All the stock solutions were stored at -20 °C. The compound list with their calibration concentrations can be found in **Supplementary Table 2**.

2.3 Sample collection and preparation

Fasted EDTA plasma samples were collected from 40 participants in the Leiden Longevity Study cohort which was enrolled between 2002 and 2006 [17]. The samples for the current study were collected at the third visit between 2009 and 2010 and stored at -80°C. The Leiden Longevity Study protocol (P09.140) was approved by the Medical Ethical Committee of the Leiden University Medical Center before the start of the study at 5th of August 2009. The first participant was enrolled at 24th of August 2009. In accordance with the Declaration of Helsinki, the Leiden Longevity Study obtained informed consent from all participants prior to their entering the study. 5 µL was taken from each plasma sample and pooled together to create a quality control (QC) sample used during method validation and bioanalysis. All plasma samples remained at -80°C until extraction.

Plasma samples, calibration samples, and QCs were thawed on ice before liquid-liquid extraction (LLE). To 5 µL plasma (or calibrant solution), 5 µL antioxidant solution, 5 µL 80 nM ISTD, 5 µL buffer solution containing 0.2 M citric acid, and 0.4 M phosphate at pH 4.5 were added in a 0.5 mL Eppendorf tube. After adding 100 µL BuOH: MTBE (1:1, v/v) and 50 µL water, oxylipins were extracted to the upper layer. Subsequently the samples were settled on ice for 20 minutes. This will facilitate the LLE because the protein layer will become more compact. After that, the samples were brought to a bullet blender to be thoroughly mixed for 4 minutes at the speed level 9. Samples were then centrifuged for 10 min at 15800 rcf under 4°C. 85 µL of the organic upper layer was collected and evaporated to dryness. Samples were reconstituted in a 20 µL mixture of MeOH: H_2O (2:8, v/v) before injection.

2.4 Micro-LC-MS/MS instrumentation and conditions

The micro-LC-MS/MS analyses were performed using a Waters nanoAcquity LC system (Waters, Milford, Massachusetts, United States) coupled to a Sciex triple quad 7500 mass spectrometer (SCIEX, Framingham, Massachusetts, United States). A Sciex Optiflow

ionization source was equipped on the MS with a SteadySpray Low Micro Electrode (1 - 50 µL/min). The separation was carried out using a Phenomenex Kinetex C18 column (2.6 µm, 150 × 0.3 mm) maintained at 40 ℃. The injection volume was 3 µL. Mobile phase A consisted of 0.1% acetic acid in water, mobile phase B was 0.1% acetic acid in a mixure of 90% ACN and 10% MeOH. Using a flow rate of 4 µL/min, the initial gradient started at 20% eluent-B and maintained for 5.0 min, eluent-B was ramped to 26% until 5.4 min, and further to 34% at 15.5 min, remained at 34% for 2 min and increased to 40% at 19.5 min, to 54% at 23.5 min, to 56% at 27.5 min, to 78% at 29.5 min, to 85% at 31.5 min, at last eluent B dropped back to 20% for re-equilibration until 40.0 min. MS data was acquired in negative ionization mode with curtain gas flow rate 32 psi, gas 1 flow rate 10 psi, gas 2 flow rate 20 psi, interface voltage at -3500 V, interface temperature at 200 °C. SRM was used for data acquisition by monitoring the precursor-product ion transitions as indicated in **Supplemental Table 3**. These instrumental conditions were used during method validation and application to plasma samples.

2.5 Method validation

Linearity and limit of detection To assess linearity, calibration lines (n = 3) were prepared over three consecutive days, incorporating a minimum of seven calibration points for each compound. All calibration lines were fitted to a 1/x2 weighted linear regression model. The limits of detection (LOD) and limits of quantification (LOQ) were calculated using the formulas LOD = 3 × S_a/b and LOQ = 10 × S_a/b, respectively. Here, S_a represents the standard deviation of the y-intercept, b represents the slope of the calibration curve.

Precision The intra- and interday precisions were evaluated by spiking three different concentrations of ISTD solutions [low-level (0.2 nM), medium-level (2.0 nM) and high-level (20 nM)] into pooled plasma samples over three different days (n = 3). Precision was expressed as the RSD of the peak areas of ISTD. An RSD less than 15% was within the tolerance limits of the EMA guidelines [18].

Recovery and matrix effects Recovery was investigated by spiking ISTD solution before LLE and after LLE. Matrix effect was evaluated by spiking ISTD solutions to pooled plasma samples (n = 3) or water (n = 3). Recovery was calculated as the ratio of ISTD peak

areas spiked before and after extraction. The Matrix effect was determined by calculating the ratio of the peak areas of ISTD spiked in pooled plasma and water samples.

2.6 Comparison to conventional UHPLC-MS/MS method

The performance of the optimized micro-LC-MS/MS method was compared to a conventional UHPLC-MS/MS described in a previous study [16]. The sample preparation procedure and starting volume (5 µL plasma) were same in both methods as described in **section 2.3**. A Shimadzu Nexera X2 LC-30AD system (Shimadzu corporation., Kyoto, Japan) was coupled to a SCIEX triple quad 7500 mass spectrometer (SCIEX, Framingham, Massachusetts, United States). An OptiFlow ionization source with spray emitters for high flow (>200 µL/min) was employed. The separation was carried out on a Waters Acquity® BEH C18 column (50 mm × 2.1 mm, 1.7 µm) maintained at 40 °C with a 5-µL injection volume. The detailed UHPLC gradient can be found in **Supplementary table 4**. MS data was acquired in negative ionization mode with curtain gas flow rate of 45 psi, gas 1 flow rate of 65 psi, gas 2 flow rate of 65 psi, interface voltage of -4500 V, interface temperature of 600 °C.

2.7 Data preprocessing

SCIEX OS version 1.6 (SCIEX, United States) was used for peak integration. Absolute quantitation was calculated using the equation of the calibration curve and using the peak area ratios (peak area of targeted analyte divided by peak area of respective ISTDs).

3. Results and discussion

3.1 micro-LC-MS/MS method development

Significant sensitivity enhancement was achieved by employing a nanoAcquity LC coupled with Shimadzu 8060 MS and a homemade spray emitter under micro-level flow rate as indicated in previous study [19]. Negative mode was used for the analysis of oxylipins. However, applying a negative voltage resulted in damage to the tip of the spray emitter due to severe corona discharge. Although the discharge problem could be mitigated by moving the emitter tip away from the MS orifice, sensitivity was sacrificed in this process. To address the discharge issue while maintaining high sensitivity under micro-flow rates, we compared several MS systems and micro-flow ionization sources, including SCIEX

nanoSprayIII with a Metal TaperTip spray emitter, Shimadzu MIKRO ionization source with a homemade spray needle, and SCIEX OptiFlow with a SteadySpray electrode (**Figure 1**). All MS parameters were optimized for the optimal performance of each system. Based on its advantages in robustness and sensitivity (**Figure 2A**), a Sciex triple quad 7500 MS with the Optiflow ionization source was ultimately selected for further method development. The SteadySpray needle also provided more flexibility with its tolerance of a wide range of flow rates.

MS	 Shimadzu LCMS8060	 SCIEX Qtrap 6500 +	 SCIEX Triple quad 7500
Ionization Source	 Shimadzu MIKRO	 SCIEX nanoSprayIII	 SCIEX OptiFlow
Spray Needle	 Modified based on Shimidazu Mikros spray needle I.D. 30 µm	 New Objective, Metal TaperTip, I.D. 30 µm	SCIEX, SteadySpray Electrode Low Micro
Flow Rate	Up to 4 µL/min	Up to 4 µL/min	1 - 50 µL/min

Figure 1. Mass spectrometers, Ionization sources, and micro-flow spray needles used for performance comparison

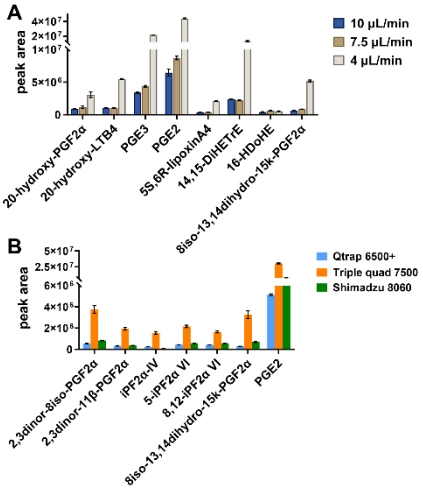

Figure 2. (A) Comparison of the performance from different MS systems using 4 µL/min; (B) optimization of micro flow rate on SCIEX triple quad 7500 MS.

To enhance the sensitivity of targeted compounds, we initially compared several flow rates. **Figure 2B** illustrates that the peak area of selected compounds increased with lower flow rate. It is also predictable that with 4 µL/min flow rate, the dilution factor of injected samples is lower. Simultaneously, a lower flow rate facilitates more efficient ionization of target compounds.

In order to improve the separation of isomers with same SRM transitions, including 8-iso-PGE2, PGE2, 11β-PGE2, PGD2 (Q1/Q3 351.1/271.2), and 8iso-15R-PGF2α, 8iso-PGF2α, 11β-PGF2α, PGF2α (Q1/Q3 353.1/193.1), a 15-cm length Phenomenex Kinetex C18 column was used. In addition, a 5-min isocratic time at the beginning of the gradient with 80% mobile phase A was applied. This step is also crucial to prevent peak tailing in early eluting compounds, such as 20-hydroxy-PGE2 and 20-hydroxy-PGF2α (**Supplementary Figure 1**).

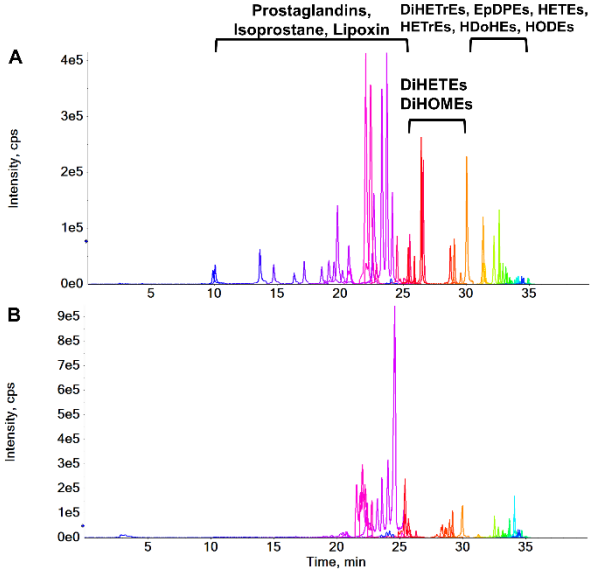

Figure 3. Overlay of SRM chromatograms of oxylipins obtained with the injection of (A) standard solution C7 and (B) 5 µL pooled plasma

Following the optimization of micro-LC-MS/MS conditions, all targeted compounds exhibited excellent resolution using a Phenomenex Kinetex C18 (2.6 µm, 0.3 × 150 mm) column with a 40-minute analysis time. The injection volume was set at 3 µL. Typical SRM

chromatograms of targeted oxylipins in standard solution and pooled human plasma are shown in **Figure 3**. Prostaglandins, isoprostane, and lipoxins eluted before 30 min, while dihydroxy- eicosatrienoic acids (DiHETrEs), epoxy- docosapentaenoic acid (EpDPEs), hydroxy- eicosatrienoic acid (HETrEs), and hydroxyeicosatetraenoic acids (HETEs) with lower polarity eluted between 30 min to 35 min. The optimized condition ensures robust analysis of the diverse oxylipin classes.

3.2 Sensitivity enhancement compared to a UHPLC-MS/MS method

The sensitivity enhancement of micro-LC-MS/MS method was evaluated by comparing its LODs and LOQs with those of conventional UHPLC-MS/MS using calibration solutions. 5 µL extracted sample was injected on a Waters Acquity® BEH C18 column (50 mm × 2.1 mm, 1.7 µm) for conventional method, and 3 µL was injected on a Phenomenex Kinetex C18 column (2.6 µm , 150 × 0.3 mm) for micro-LC-MS/MS method. The same MS and ionization source were utilized for a fair comparison. In **Figure 4**, the fold changes in LOD and LOQ for the micro flow method over the conventional method are depicted for targeted oxylipins. For 13-HODE, 8,12-iPF2α-VI, and 13,14-dihydro-15keto-PGE2, the calibration points within the same concentration ranges of the micro-LC-MS method were insufficient for calculating LOD and LOQ compared with the UHPLC-MS/MS method.

Among the other 63 oxylipins, sensitivity increased from 1.4 to 180.7 times in 51 compounds (orange bars in **Figure 4**). However, due to differences in the compounds physical-chemical properties, for 10 compounds (depicted as green bars in **Figure 4**), including 9-HETE, 11-HDoHE, 10-HDoHE, 9-HODE, 16-HDoHE, 5-HEPE, 12-HETE, 17-HDoHE, 20-HDoHE, and 8-HDoHE, micro-LC-MS performance was found to be inferior to that of the UHPLC-MS/MS method. Different reconstitution solvents and LC gradients were used for the micro-LC-MS and UHPLC-MS methods, resulted in change of chromatographic selectivity, and lead to changes in ion suppression for those compounds due to the matrix effect. The ion suppression subsequently resulted in higher LOD and lower signal to noise ratio for micro-LC-MS. For detailed LOD and LOQ values for both methods, refer to **Supplementary table 5**.

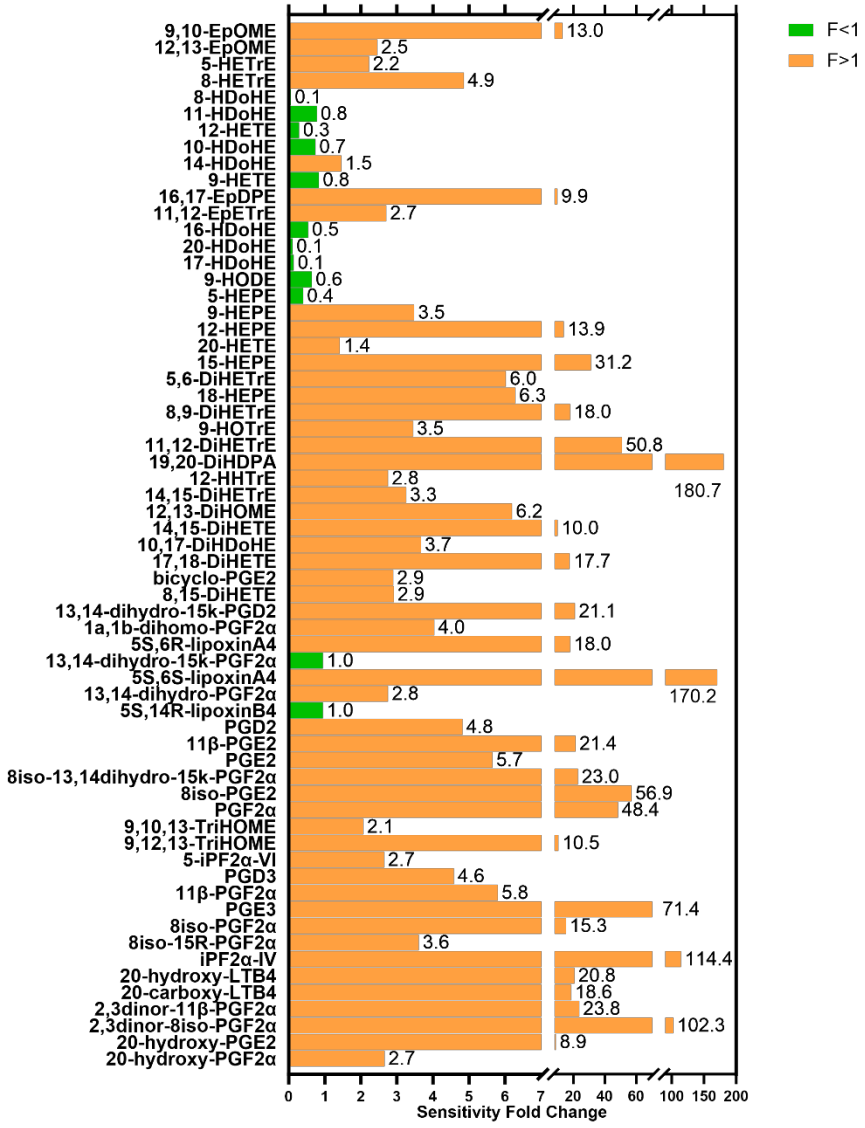

Figure 4. Sensitivity fold change (F) calculated by LOD (LOQ) of micro-LC-MS/MS divided by LOD (LOQ) from UHPLC-MS/MS, compounds arranged in elution order from bottom to top.

3.3 Method validation

The optimized method outlined in **Section 2.4** was validated with the evaluation of linearity, precision, recovery and matrix effects. To cater to the demands of quantification in 5 µL

human plasma, the calibration solutions were diluted to picomolar level near the detection limits.

The linearity of all compounds was established using calibrant solutions, yielding coefficient of determination (R^2) values ranging from 0.9930 to 0.9999. Back-calculated concentrations of the calibration standards fell within ±15% (20% for LOQ) of the nominal values, indicating satisfactory linearity for all analytes. The LOQs were determined to be between 0.3 pM and 306.2 pM, as summarized in **Table 1**.

Table 1. Validation parameters: calibration range, LODs, and LOQs.

Compound name	Linearity range (nM)	R^2	LOD (pM)	LOQ (pM)
20-hydroxy-PGF2α	0.12 -29.93	0.9976	1.9	6.2
20-hydroxy-PGE2	0.02 -21.3	0.9986	0.3	1.0
2,3dinor-8iso-PGF2α	0.07 -37.5	0.9996	0.3	1.1
20-carboxy-LTB4	0.08 -20.63	0.9988	1.3	4.2
2,3dinor-11β-PGF2α	0.07 -37.5	0.9989	1.2	4.1
20-hydroxy-LTB4	0.04 -20.85	0.9987	0.8	2.6
iPF2α-IV	0.07 -37.5	0.9979	0.2	0.8
8iso-15R-PGF2α	0.07 -37.5	0.9994	0.8	2.8
8iso-PGF2α	0.07 -37.5	0.9995	2.1	6.8
11β-PGF2α	0.12 -29.63	0.9989	1.1	3.8
PGF2α	0.04 -37.5	0.9991	0.2	0.8
PGE3	0.04 -37.5	0.9989	0.1	0.3
PGD3	0.04 -37.5	0.9991	0.6	1.8
8iso-PGE2	0.04 -37.5	0.9994	0.1	0.3
PGE2	0.04 -37.5	0.9988	0.9	2.9
11β-PGE2	0.03 -29.78	0.9995	0.3	0.9
PGD2	0.04 -37.5	0.9990	0.4	1.3
5-iPF2α -VI	0.15 -37.5	0.9989	2.5	8.3
8,12-iPF2α-VI	1.17 -37.5	0.9991	23.0	76.5
9,12,13-TriHOME	0.12 -30.11	0.9988	6.6	22.0
9,10,13-TriHOME	0.06 -30.11	0.9990	4.6	15.4
8iso-13,14dihydro-15keto-PGF2α	0.15 -37.5	0.9996	1.1	3.6
13,14dihydro-15keto-PGF2α	0.12 -14.81	0.9984	2.5	8.5
13,14dihydro-PGF2α	0.03 -14.74	0.9987	3.5	11.7
13,14dihydro-15keto-PGE2	0.03 -14.89	0.9996	0.3	0.9
13,14dihydro-15keto-PGD2	0.03 -29.78	0.9993	0.3	1.1
5S,6R-lipoxinA4	0.04 -20.85	0.9993	1.0	3.4
5S,6S-lipoxinA4	0.02 -10.43	0.9987	0.1	0.3
1a,1b-dihomo-PGF2α	0.03 -27.45	0.9993	0.6	2.1
bicyclo-PGE2	0.03 -31.43	0.9991	0.9	3.0
8,15-DiHETE	0.33 -20.93	0.9985	6.1	20.5
10,17-DiHDoHE	0.16 -21	0.9984	4.7	15.8
17,18-DiHETE	0.12 -30	0.9991	2.4	8.0
14,15-DiHETE	0.03 -30	0.9989	0.7	2.3
12,13-DiHOME	0.16 -41.4	0.9986	2.3	7.6
14,15-DiHETrE	0.02 -21.08	0.9988	0.9	3.0
12-HHTrE	0.02 -21	0.9989	4.4	14.7
19,20-DiHDPA	0.02 -20.85	0.9987	0.1	0.4
11,12-DiHETrE	0.02 -10.54	0.9991	0.1	0.4
9-HOTrE	0.04 -21.41	0.9982	2.6	8.8

Compound name	Linearity range (nM)	R^2	LOD (pM)	LOQ (pM)
8,9-DiHETrE	0.02 -21	0.9986	0.5	1.6
18-HEPE	0.09 -11.55	0.9975	3.0	9.9
15-HEPE	0.04 -21.15	0.9983	0.4	1.5
20-HETE	0.08 -21	0.9965	8.8	29.3
5,6-DiHETrE	0.16 -10.54	0.9973	2.2	7.4
12-HEPE	0.17 -21.15	0.9957	0.4	1.5
9-HEPE	0.18 -11.55	0.9948	3.9	12.9
13-HODE	1.33 -42.53	0.9981	59.0	196.6
12,13-EpOME	0.16 -20.55	0.9984	4.3	14.4
5-HEPE	0.17 -10.58	0.9978	5.7	19.1
9-HODE	0.66 -21.26	0.9981	27.7	92.3
9,10-EpOME	0.08 -20.55	0.9984	2.2	7.3
17-HDoHE	1.34 -21.38	0.9936	47.3	157.6
20-HDoHE	1.34 -21.38	0.9832	91.9	306.2
16-HDoHE	0.33 -21	0.9982	3.4	11.5
16,17-EpDPE	0.17 -10.69	0.9967	5.1	16.8
9-HETE	0.48 -30.53	0.9970	8.3	27.8
11,12-EpETrE	0.33 -21	0.9968	0.6	1.8
14-HDoHE	0.04 -5.25	0.9946	7.1	23.6
10-HDoHE	0.33 -21.38	0.9980	12.8	42.6
12-HETE	0.17 -21.38	0.9942	21.9	72.9
11-HDoHE	0.66 -21	0.9944	8.8	29.2
8-HDoHE	0.33 -21.38	0.9964	76.4	254.6
8-HETrE	1.34 -21.38	0.9981	4.4	14.5
5-HETrE	0.18 -22.8	0.9961	4.7	15.6
5S,14R-lipoxinB4	0.18 -22.8	0.9972	11.6	38.6

Intra- and interday precisions varied from 0.5% to 11.7% and from 2.5% to 14.1%, respectively. All values were within the 15% tolerance limit, underscoring the repeatability of the method, as detailed in **Table 2**.

Table 2. Intraday and interday precision (RSD%) of oxylipins spiked to plasma

Compounds	**Intraday precision (%)**			**Interday precision (%)**		
	Low	**Medium**	**High**	**Low**	**Medium**	**High**
d_4-8iso-PGF2α	11.4	9.6	5.2	5.8	6.0	3.5
d_4-PGF2α	14.1	3.6	6.3	2.3	4.9	2.8
d_{11}-5-iPF2α-VI	9.6	8.0	6.2	2.9	2.5	5.5
d_{11}-8,12-iso-iPF2α-VI	2.5	4.5	3.5	2.9	4.2	3.6
d_4-8iso-PGE2	5.8	2.9	3.7	2.0	1.2	1.7
d_4-PGE2	14.1	3.6	4.6	7.4	4.0	3.4
d_4-PGD2	7.1	6.5	6.9	1.5	2.1	2.9
d_9-PGE2	2.5	2.6	5.9	1.0	1.4	0.7
d_4-LTB4	7.1	5.3	9.0	1.6	1.4	0.7
d_4-12,13-DiHOME	8.7	6.0	9.0	11.7	2.8	4.3
d_4-9,10-DiHOME	5.8	6.6	2.6	1.7	1.3	1.8
d_{11}-14,15-DiHETrE	4.3	8.7	7.4	0.5	3.3	2.3
d_6-20-HETE	13.5	6.8	12.1	9.8	10.0	12.5

Matrix effect suggests ion enhancement or suppression during MS ionization due to matrix components. Matrix effects above 100% indicate ion enhancement, suggesting that components in the matrix positively influence the ionization of analytes, leading to higher signal intensities. Conversely, matrix effects below 100% suggest ion suppression, where the matrix components hinder the ionization of analytes, resulting in reduced signal intensities. Deuterated internal standards were employed for the determination of recovery and matrix effect. The recoveries ranged from 64.6% to 99.6%. Matrix effect ranged from 79.2% to 130.3% (**Figure 5**). Particularly, ion enhancement was observed in LTB4-d4. All compounds demonstrated acceptable recovery rates and consistent matrix effects across three concentration levels, affirming the applicability of the sample preparation method for quantitative analysis. The results collectively emphasize the robustness and reliability of the validated method for the sensitive and accurate quantification of oxylipins in volume-limited human plasma.

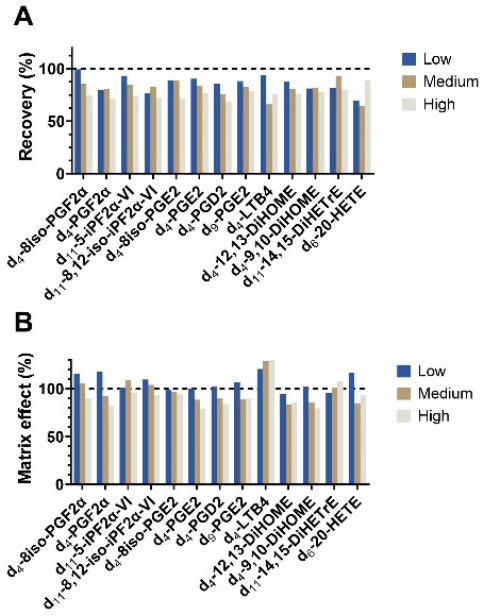

Figure 5. Recovery and matrix effect of deuterated internal standards in human plasma. Recovery and matrix effect values are expressed in percentages. (A) Recovery: higher values indicate better recoveries. (B) Matrix effect: values above 100% indicate ion enhancement and below 100% imply ion suppression.

3.4 Application in a sample-limited clinical study modeling healthy aging

The validated method was applied to a healthy aging study involving 40 human plasma samples grouped by genders. Three samples were excluded due to technical errors. 4 pooled plasma samples were analyzed along with the study samples as QC samples. Compounds with >80% missing values in study samples or >50% missing values in QCs were also excluded for data reliability. As presented in **Table 3**, a total of 28 oxylipins were successfully quantified in study samples, revealing a broad concentration range spanning from 51.8±21.8 pM (8,9-DiHETrE in male samples) to 30.9 ± 8.9 nM (13-HODE). These findings underscore the applicability of the developed micro-LC-MS/MS method in analyzing oxylipins within volume-limited plasma samples, particularly in the context of studies focused on healthy aging. It is worth noting that the current results serve as a promising indication of the method's suitability for oxylipin studies in volume-limited plasma, given the diverse range of concentrations successfully determined.

Table 3. Average concentrations of oxylipins in two groups of study samples (Mean ± SD)

Oxylipins	Female (n=18, pM)	Male (n=19, pM)
5-iPFα-VI	152±73	153±80
8,12-iso-iPF2α-VI	4115±1930	4258±1920
9,12,13-TriHOME	1241±737	2297±1725
9,10,13-TriHOME	230±184	227±102
17,18-DiHETE	2014±896	1922±765
14,15-DiHETE	267±121	243±81
12,13-DiHOME	3373±1900	3845±1816
14,15-DiHETrE	148±49	147±30
12-HHTrE	71±20	206±319
19,20-DiHDPA	468±182	473±252
11,12-DiHETrE	124±41	120±31
9-HOTrE	1052±638	850±407
8,9-DiHETrE	64±26	52±22
18-HEPE	135±63	127±61
15-HEPE	148±91	119±29
20-HETE	306±154	243±90
5,6-DiHETrE	196±80	198±107
12-HEPE	71±41	100±84

Oxylipins	Female (n=18, pM)	Male (n=19, pM)
13-HODE	30852±8892	29356±11859
12,13-EpOME	2239±1534	2011±806
5-HEPE	302±346	317±137
9-HODE	20316±7779	23773±13832
9,10-EpOME	475±314	427±179
20-HDoHE	779±624	543±278
16-HDoHE	191±218	142±61
16,17-EpDPE	341±135	353±169
11,12-EpETrE	170±55	181±73
8-HETrE	181±69	162±65

4. Conclusion

In this study, we developed a micro-LC-MS/MS method tailored for the precise determination of oxylipins in volume-limited human plasma. Requiring only 5 μL plasma, the method achieved LODs ranging from 0.1 pM to 91.9 pM, and LOQs ranging from 0.3 pM to 306.2 pM. The method exhibited good repeatability, with intraday and interday precisions consistently below 14.1%. To assess its sensitivity enhancement, the developed micro-LC-MS/MS method underwent a thorough comparison with a conventional flow UHPLC-MS/MS method. The results demonstrated that our method is not only sensitive but also well-suited for bioanalysis in volume-limited plasma. We subsequently applied the validated method to analyze 40 human plasma samples for oxylipin determination. Although the difference between the two gender groups is not significant among current sample set, the method is robust and could contribute to cohort studies with volume-limited samples. With the wide coverage of concentration levels in different oxylipins and robustness for plasma analysis, our method is instrumental in its ability for future research in oxylipins, especially when confronted with volume-limited samples. To pave the way for its broader utility in clinical and research settings, further development of the method should prioritize expanding the targets to other signaling lipids such as fatty acids, bile acids, etc., and evaluating its performance in extensive sample cohorts under diverse health conditions.

Declaration of Competing Interest

The authors declare that they have no known competing financial interests or personal relationships that could have appeared to influence the work reported in this paper.

Acknowledgements

The authors would like to thank Faisa Guled for valuable discussions and technical assistance with the laboratory work. This research was supported by DuSRA-VOILA (Vitality Oriented Innovation for the Lifecourse of the Ageing Society), project number 457001001. The construction and maintenance of the Leiden Longevity Study biomaterial and data has received funding from the European Union's Seventh Framework Programme (FP7/2007-2011; grant agreement number 259679), the Innovation-Oriented Research Program on Genomics (SenterNovem IGE05007), and the Netherlands Consortium for Healthy Ageing (050-060-810). Dr. Amy Harms would like to acknowledge the financial support from The Netherlands X-omics Initiative NWO (project 184.034.019). This study was also supported by the China Scholarship Council (CSC, No. 201906390032 to Bingshu He) and the Vidi grant scheme of the Dutch Research Council (NWO Vidi 723.016.003 to Rawi Ramautar).

References

[1] M. Misheva, J. Johnson, J. McCullagh, Role of Oxylipins in the Inflammatory-Related Diseases NAFLD, Obesity, and Type 2 Diabetes, Metabolites, 12 (2022) 1238.
[2] M.A. Nayeem, Role of oxylipins in cardiovascular diseases, Acta Pharmacologica Sinica, 39 (2018) 1142-1154.
[3] Á. Jara-Gutiérrez, V. Baladrón, The Role of Prostaglandins in Different Types of Cancer, Cells, 10 (2021) 1487.
[4] U.N. Das, Essential Fatty Acids and Their Metabolites in the Pathobiology of Inflammation and Its Resolution, Biomolecules, 11 (2021) 1873.
[5] G.L. Milne, Q. Dai, L.J. Roberts, The isoprostanes—25 years later, Biochimica et Biophysica Acta (BBA) - Molecular and Cell Biology of Lipids, 1851 (2015) 433-445.
[6] I. Ferreira, F. Falcato, N. Bandarra, A.P. Rauter, Resolvins, Protectins, and Maresins: DHA-Derived Specialized Pro-Resolving Mediators, Biosynthetic Pathways, Synthetic Approaches, and Their Role in Inflammation, Molecules, 27 (2022) 1677.
[7] D.E. Le, M. García-Jaramillo, G. Bobe, A. Alcazar Magana, A. Vaswani, J. Minnier, D.B. Jump, D. Rinkevich, N.J. Alkayed, C.S. Maier, S. Kaul, Plasma Oxylipins: A Potential Risk Assessment Tool in Atherosclerotic Coronary Artery Disease, Frontiers in Cardiovascular Medicine, 8 (2021).
[8] X. Fu, M. Anderson, Y. Wang, J.C. Zimring, LC-MS/MS-MRM-Based Targeted Metabolomics for Quantitative Analysis of Polyunsaturated Fatty Acids and Oxylipins, in: A. D'Alessandro (Ed.) High-Throughput Metabolomics: Methods and Protocols, Springer New York, New York, NY, 2019, pp. 107-120.

[9] T. Wang, H. Li, Y. Han, Y. Wang, J. Gong, K. Gao, W. Li, H. Zhang, J. Wang, X. Qiu, T. Zhu, A rapid and high-throughput approach to quantify non-esterified oxylipins for epidemiological studies using online SPE-LC-MS/MS, Analytical and Bioanalytical Chemistry, 412 (2020) 7989-8001.
[10] K. Strassburg, A.M.L. Huijbrechts, K.A. Kortekaas, J.H. Lindeman, T.L. Pedersen, A. Dane, R. Berger, A. Brenkman, T. Hankemeier, J. van Duynhoven, E. Kalkhoven, J.W. Newman, R.J. Vreeken, Quantitative profiling of oxylipins through comprehensive LC-MS/MS analysis: application in cardiac surgery, Analytical and Bioanalytical Chemistry, 404 (2012) 1413-1426.
[11] I. Liakh, A. Pakiet, T. Sledzinski, A. Mika, Methods of the Analysis of Oxylipins in Biological Samples, Molecules, 25 (2020) 349.
[12] W. Jung, C.H. Ahn, A micro blood sampling system for catheterized neonates and pediatrics in intensive care unit, Biomedical Microdevices, 15 (2013) 241-253.
[13] J. Kovač, G. Panic, A. Neodo, I. Meister, J.T. Coulibaly, J.D. Schulz, J. Keiser, Evaluation of a novel micro-sampling device, Mitra™, in comparison to dried blood spots, for analysis of praziquantel in Schistosoma haematobium-infected children in rural Côte d'Ivoire, Journal of Pharmaceutical and Biomedical Analysis, 151 (2018) 339-346.
[14] N.A. Karp, L. Coleman, P. Cotton, N. Powles-Glover, A. Wilson, Impact of repeated micro and macro blood sampling on clinical chemistry and haematology in rats for toxicokinetic studies, Regulatory Toxicology and Pharmacology, 141 (2023) 105386.
[15] M. Cebo, X. Fu, M. Gawaz, M. Chatterjee, M. Lämmerhofer, Micro-UHPLC-MS/MS method for analysis of oxylipins in plasma and platelets, Journal of Pharmaceutical and Biomedical Analysis, 189 (2020) 113426.
[16] W. Yang, J.C. Schoeman, X. Di, L. Lamont, A.C. Harms, T. Hankemeier, A comprehensive UHPLC-MS/MS method for metabolomics profiling of signaling lipids: Markers of oxidative stress, immunity and inflammation, Analytica Chimica Acta, 1297 (2024) 342348.
[17] R.G.J. Westendorp, D. Van Heemst, M.P. Rozing, M. Frölich, S.P. Mooijaart, G.-J. Blauw, M. Beekman, B.T. Heijmans, A.J.M. De Craen, P.E. Slagboom, f.t.L.L.S. Group, Nonagenarian Siblings and Their Offspring Display Lower Risk of Mortality and Morbidity than Sporadic Nonagenarians: The Leiden Longevity Study, Journal of the American Geriatrics Society, 57 (2009) 1634-1637.
[18] E.E.M. Agency, Guidlines for the validation of analytical methods used in residue depletion studies, in: E.M. Agency (Ed.), 2009.
[19] B. He, X. Di, F. Guled, A.V.E. Harder, A.M.J.M. van den Maagdenberg, G.M. Terwindt, E.H.J. Krekels, I. Kohler, A. Harms, R. Ramautar, T. Hankemeier, Quantification of endocannabinoids in human cerebrospinal fluid using a novel micro-flow liquid chromatography-mass spectrometry method, Analytica Chimica Acta, 1210 (2022) 339888.

Supporting Information

Supplementary Table 1. Abbreviations and purchasing information of oxylipins and labeled standards

Abbr.	Common Name	Systematic name	Molecular formula	Cayman	CAS	Mass	HMDB
20-hydroxy-PGF2α	20-hydroxy Prostaglandin F2α	9α,11α,15S,20-tetrahydroxy-prosta-5Z,13E-dien-1-oic acid	$C_{20}H_{34}O_6$	16950	57930-92-4	370.2355	HMDB0004049
20-hydroxy-PGE2	20-Hydroxy-PGE2	9-oxo-11α,15S,20-trihydroxy-prosta-5Z,13E-dien-1-oic acid	$C_{20}H_{32}O_6$	14950	57930-95-7	368.2199	HMDB0003247
2,3-dinor-8-iso-PGF2α	2,3-dinor-8-iso Prostaglandin F2α	9α,11α,15S-trihydroxy-2,3-dinor-(8β)-prosta-5Z,13E-dien-1-oic acid	$C_{18}H_{30}O_5$	16290	221664-05-7	326.4000	NA
20-carboxy-LTB4	20-Carboxy-leukotriene B4	5S,12R-dihydroxy-6Z,8E,10E,14Z-eicosatetraene-1,20-dioic acid	$C_{20}H_{30}O_6$	20180	80434-82-8	366.2042	HMDB0006059
2,3-dinor-11β-PGF2α	2,3-dinor-11β-Prostaglandin F2α	9α,11β,15S-trihydroxy-2,3-dinor-prosta-5Z,13E-dien-1-oic acid	$C_{18}H_{30}O_5$	16530	240405-20-3	326.4000	NA
20-hydroxy-LTB4	20-Hydroxy-leukotriene B4	5S,12R,20-trihydroxy-6Z,8E,10E,14Z-eicosatetraenoic acid	$C_{20}H_{32}O_5$	20190	79516-82-8	352.2249	HMDB0001509
iPF2α-IV	iPF2alpha-IV	(8S)-10-[(1R,2S,3S,5R)-3,5-Dihydroxy-2-pentylcyclopentyl]-8-hydroxydeca-5,9-dienoic acid	$C_{20}H_{34}O_5$		331962-00-6	354.2000	NA
8-iso-15-R-PGF2α	8-iso-15(R)-Prostaglandin F2α	9α,11α,15R-trihydroxy-(8β)-prosta-5Z,13E-dien-1-oic acid	$C_{20}H_{34}O_5$	16395	214748-65-9	354.2406	NA
8-iso-PGF2a	8-iso-15(S)-Prostaglandin F2α	9α,11α,15S-trihydroxy-(8β)-prosta-5Z,13E-dien-1-oic acid	$C_{20}H_{34}O_5$	16350	27415-26-5	354.2406	HMDB0005083
11β-PGF2a	11β-Prostaglandin F2α	9α,11β,15S-trihydroxy-prosta-5Z,13E-dien-1-oic acid	$C_{20}H_{34}O_5$	16520	38432-87-0	354.2406	NA
PGF2α	Prostaglandin F2α	9α,11α,15S-trihydroxy-prosta-5Z,13E-dien-1-oic acid	$C_{20}H_{34}O_5$	16010	551-11-1	354.2406	HMDB0001139
PGE3	Prostaglandin E3	9-oxo-11α,15S-dihydroxy-prosta-5Z,13E,17Z-trien-1-oic acid	$C_{20}H_{30}O_5$	14990	802-31-3	350.2093	HMDB0002664
PGD3	Prostaglandin D3	9α,15S-dihydroxy-11-oxo-prosta-5Z,13E,17Z-trien-1-oic acid	$C_{20}H_{30}O_5$	12990	71902-47-1	350.2093	HMDB0003034
8-iso-PGE2	8-iso Prostaglandin E2	9-oxo-11α,15S-dihydroxy-(8β)-prosta-5Z,13E-dien-1-oic acid	$C_{20}H_{32}O_5$	14350	27415-25-4	352.2250	HMDB0005844
PGE2	Prostaglandin E2	9-oxo-11α,15S-dihydroxy-prosta-5Z,13E-dien-1-oic acid	$C_{20}H_{32}O_5$	14010	363-24-6	352.2250	HMDB0001220
11β-PGE2	11β-Prostaglandin E2	9-oxo-11β,15S-dihydroxy-prosta-5Z,13E-dien-1-oic acid	$C_{20}H_{32}O_5$	14510	38310-90-6	352.2250	HMDB0060041
PGD2	Prostaglandin D2	9α,15S-dihydroxy-11-oxo-prosta-5Z,13E-dien-1-oic acid	$C_{20}H_{32}O_5$	12010	41598-07-6	352.2250	HMDB0001403

Abbr.	Common Name	Systematic name	Molecular formula	Cayman	CAS	Mass	HMDB
5-iPF2α VI	(±)5-iPF2α-VI	(8β)-5,9α,11α-trihydroxy-prosta-6E,14Z-dien-1-oic acid	$C_{20}H_{34}O_5$	16300	179094-11-2	354.2406	NA
8,12-iPF2α VI	8,12-iso-iPF2α-VI-1,5-lactone	6-((E)-2-((1R,2S,3R,5S)-3,5-dihydroxy-2-((Z)-oct-2-enyl) cyclopentyl) vinyl) tetrahydro-2H-pyran-2-one	$C_{20}H_{32}O_4$	10312		336.5000	NA
9,12,13-TriHOME	9(S),12(S),13(S)-TriHOME	9S,12S,13S-trihydroxy-11E-octadecenoic acid	$C_{18}H_{34}O_5$	10005143	97134-11-7	330.2406	HMDB0004708
9,10,13-TriHOME	9(S),10(S),13(S)-TriHOME	9S,10S,13S-trihydroxy-11E-octadecenoic acid	$C_{18}H_{34}O_5$	26768	135214-44-7	330.2406	
8-iso-13,14-dihydro-15-keto-PGF2α	8-iso-13,14-dihydro-15-keto Prostaglandin F2α	9α,11α-dihydroxy-15-oxo-(8β)-prost-5Z-en-1-oic acid	$C_{20}H_{34}O_5$	16380	191919-02-5	354.2406	HMDB0006562
13,14-dihydro-15-keto-PGF2α	13,14-dihydro-15-keto Prostaglandin F2α	9α,11α-dihydroxy-15-oxo-prost-5Z-en-1-oic acid	$C_{20}H_{34}O_5$	16670	27376-76-7	354.2406	HMDB0004685
13,14-dihydro-PGF2α	13,14-dihydro Prostaglandin F2α	9α,11α,15S-trihydroxy-prost-5Z-en-1-oic acid	$C_{20}H_{36}O_5$	16660	27376-74-5	356.2563	HMDB0004239
13,14-dihydro-15-keto-PGE2	13,14-dihydro-15-keto Prostaglandin E2	9,15-dioxo-11α-hydroxy-prost-5Z-en-1-oic acid	$C_{20}H_{32}O_5$	14650	363-23-5	352.2250	HMDB0002776
13,14-dihydro-15-keto-PGD2	13,14-dihydro-15-keto Prostaglandin D2	9α-hydroxy-11,15-dioxo-prost-5Z-en-1-oic acid	$C_{20}H_{32}O_5$	12610	59894-07-4	352.2250	HMDB0060042
5S,6R-lipoxinA4	Lipoxin A4	5S,6R,15S-trihydroxy-7E,9E,11Z,13E-eicosatetraenoic acid	$C_{20}H_{32}O_5$	90410	89663-86-5	352.2250	HMDB0004385
5S,6S-lipoxinA4	6(S)-Lipoxin A4	5S,6S,15S-trihydroxy-7E,9E,11Z,13E-eicosatetraenoic acid	$C_{20}H_{32}O_5$	10049	94292-80-5	352.2250	NA
1a,1b-dihomo-PGF2α	1a,1b-dihomo Prostaglandin F2α	9α,11α,15S-trihydroxy-1a,1b-dihomo-prosta-5Z,13E-dien-1-oic acid	$C_{22}H_{38}O_5$	16050	57944-39-5	382.2719	NA
bicyclo-PGE2	Bicyclo Prostaglandin E2	11-deoxy-13,14-dihydro-15-keto-11β,16.xi.-cycloprostaglandin E2	$C_{20}H_{30}O_4$	14530	74158-09-1	334.2144	HMDB0060054
8,15-DiHETE	8(S),15(S)-DiHETE	8S,15S-dihydroxy-5Z,9E,11Z,13E-eicosatetraenoic acid	$C_{20}H_{32}O_4$	35370	80234-65-7	336.5000	NA
10,17-DiHDoHE	10(S),17(S)-DiHDHA	10(S),17(S)-dihydroxy-4Z,7Z,11E,13Z,15E,19Z-docosahexaenoic acid	$C_{22}H_{32}O_4$	10008128	871826-47-0	360.2301	NA
17,18-DiHETE	(±)17(18)-DiHETE	(±)17,18-dihydroxy-5Z,8Z,11Z,14Z-eicosatetraenoic acid	$C_{20}H_{32}O_4$	10006999		336.2301	HMDB0010211
14,15-DiHETE	(±)14(15)-DiHETE	(±)14,15-dihydroxy-5Z,8Z,11Z,17Z-eicosatetraenoic acid	$C_{20}H_{32}O_4$	10006998		336.2301	HMDB0010204
12,13-DiHOME	(±)12(13)-DiHOME	(±)12,13-dihydroxy-9Z-octadecenoic acid	$C_{18}H_{34}O_4$	10009832	263399-35-5	314.2457	HMDB0004705
14,15-DiHETrE	(±)14(15)-DiHET	(±)14,15-dihydroxy-5Z,8Z,11Z-eicosatrienoic acid	$C_{20}H_{34}O_4$	51651	77667-09-5	338.2457	HMDB0002265

Abbr.	Common Name	Systematic name	Molecular formula	Cayman	CAS	Mass	HMDB
12-HHTrE	12(S)-HHTrE	12S-hydroxy-5Z,8E,10E-heptadecatrienoic acid	$C_{17}H_{28}O_3$	34590	54397-84-1	280.2038	HMDB0012535
19,20-DiHDPA	(±)19(20)-DiHDPA	(±)19,20-dihydroxy-4Z,7Z,10Z,13Z,16Z-docosapentaenoic acid	$C_{22}H_{34}O_4$	10007001		362.2457	HMDB0010214
11,12-DiHETrE	(±)11(12)-DiHET	(±)11,12-dihydroxy-5Z,8Z,14Z-eicosatrienoic acid	$C_{20}H_{34}O_4$	51511	192461-95-3	338.2457	HMDB0002314
9-HOTrE	9(S)-HOTrE	9S-hydroxy-10E,12Z,15Z-octadecatrienoic acid	$C_{18}H_{30}O_3$	39420	89886-42-0	294.2195	HMDB0031934
8,9-DiHETrE	(±)8(9)-DiHET	(±)8,9-dihydroxy-5Z,11Z,14Z-eicosatrienoic acid	$C_{20}H_{34}O_4$	51351	192461-96-4	338.2457	HMDB0002311
18-HEPE	(±)18-HEPE	(±)-18-hydroxy-5Z,8Z,11Z,14Z,16E-eicosapentaenoic acid	$C_{20}H_{30}O_3$	32840	141110-17-0	318.2195	HMDB0012611(R)
15-HEPE	(±)15-HEPE	(±)-15-hydroxy-5Z,8Z,11Z,13E,17Z-eicosapentaenoic acid	$C_{20}H_{30}O_3$	32700	88852-33-9	318.2195	HMDB0010209
20-HETE	(±)20-HETE	20-hydroxy-5Z,8Z,11Z,14Z-eicosatetraenoic acid	$C_{20}H_{32}O_3$	90030	79551-86-3	320.2351	HMDB0005998
5,6-DiHETrE	(±)5(6)-DiHET	(±)5,6-dihydroxy-8Z,11Z,14Z-eicosatrienoic acid	$C_{20}H_{34}O_4$	51211	213382-49-1	338.2457	HMDB0002343
12-HEPE	(±)12-HEPE	(±)-12-hydroxy-5Z,8Z,10E,14Z,17Z-eicosapentaenoic acid	$C_{20}H_{30}O_3$	32540	81187-21-5	318.2195	HMDB10202
9-HEPE	(±)9-HEPE	(±)-9-hydroxy-5Z,7E,11Z,14Z,17Z-eicosapentaenoic acid	$C_{20}H_{30}O_3$	32400	286390-03-2	318.2195	HMDB0060053
13-HODE	(±)13-HODE	(±)-13-hydroxy-9Z,11E-octadecadienoic acid	$C_{18}H_{32}O_3$	38600	18104-45-5	296.2351	HMDB0112194
12,13-EpOME	(±)12(13)-EpOME	(±)12(13)epoxy-9Z-octadecenoic acid	$C_{18}H_{32}O_3$	52450		296.2351	HMDB0004702
5-HEPE	(±)5-HEPE	(±)-5-hydroxy-6E,8Z,11Z,14Z,17Z-eicosapentaenoic acid	$C_{20}H_{30}O_3$	32200	83952-40-3	318.2195	HMDB0005081
9-HODE	(±)9-HODE	(±)-9-hydroxy-10E,12Z-octadecadienoic acid	$C_{18}H_{32}O_3$	38400	98524-19-7	296.2351	HMDB0010223
9,10-EpOME	(±)9(10)-EpOME	(±)9,10-epoxy-12Z-octadecenoic acid	$C_{18}H_{32}O_3$	52400		296.2351	HMDB0004701
17-HDoHE	(+/-)-17-HDoHE	(±)17-hydroxy-4Z,7Z,10Z,13Z,15E,19Z-docosahexaenoic acid	$C_{22}H_{32}O_3$	33650	90780-52-2	344.2351	HMDB0010213
20-HDoHE	(+/-) 20-HDoHE	(±)20-hydroxy-4Z,7Z,10Z,13Z,16Z,18E-docosahexaenoic acid	$C_{22}H_{32}O_3$	33750	90906-41-5	344.2351	HMDB0060048
16-HDoHE	(+/-) 16-HDoHE	(±)16-hydroxy-4Z,7Z,10Z,13Z,17E,19Z-docosahexaenoic acid	$C_{22}H_{32}O_3$	33600	90780-51-1	344.2351	HMDB0060047

Abbr.	Common Name	Systematic name	Molecular formula	Cayman	CAS	Mass	HMDB
16,17-EpDPE	(±)16(17)-EpDPA	(±)16,17-epoxy-4Z,7Z,10Z,13Z,19Z-docosapentaenoic acid	$C_{22}H_{32}O_3$	10174	155073-46-4	344.2351	HMDB0013621
9-HETE	(±)9-HETE	(±)-9-hydroxy-5Z,7E,11Z,14Z-eicosatetraenoic acid	$C_{20}H_{32}O_3$	34400	79495-85-5	320.2351	HMDB0010222
11,12-EpETrE	(±)11,12-EpETrE	(±)11,(12)-epoxy-5Z,8Z,14Z-eicosatrienoic acid	$C_{20}H_{32}O_3$	50511	123931-40-8	320.2351	HMDB0004673
14-HDoHE	(+/-) 14-HDoHE	(±)14-hydroxy-4Z,7Z,10Z,12E,16Z,19Z-docosahexaenoic acid	$C_{22}H_{32}O_3$	33550	87042-40-8	344.2351	HMDB0060044
10-HDoHE	(+/-) 10-HDoHE	(±)10-hydroxy-4Z,7Z,11E,13Z,16Z,19Z-docosahexaenoic acid	$C_{22}H_{32}O_3$	33400	90780-50-0	344.2351	HMDB0060037
12-HETE	(±)12-HETE	(±)12-hydroxy-5Z,8Z,10E,14Z-eicosatetraenoic acid	$C_{20}H_{32}O_3$	34550	71030-37-0	320.2351	HMDB0006111
11-HDoHE	(+/-) 11-HDoHE	(±)11-hydroxy-4Z,7Z,9E,13Z,16Z,19Z-docosahexaenoic acid	$C_{22}H_{32}O_3$			344.2351	HMDB0060040
8-HDoHE	(+/-) 8-HDoHE	(±)8-hydroxy-4Z,6E,10Z,13Z,16Z,19Z-docosahexaenoic acid	$C_{22}H_{32}O_3$	33350	90780-54-4	344.2351	HMDB0060051
8-HETrE	8(S)-HETrE	8S-hydroxy-9E,11Z,14Z-eicosatrienoic acid	$C_{20}H_{34}O_3$	36360	889573-69-7	322.2508	NA
5-HETrE	5(S)-HETrE	5S-hydroxy-6E,8Z,11Z-eicosatrienoic acid	$C_{20}H_{34}O_3$	36230	195061-94-0	322.2508	NA
5S-14R-lipoxin B4	Lipoxin B4	5S,14R,15S-trihydroxy-6E,8Z,10E,12E-eicosatetraenoic acid	$C_{20}H_{32}O_5$	90420	98049-69-5	352.2250	HMDB0005082
d_4-8iso-PGF2α	8-iso Prostaglandin F2α-d_4	9α,11α,15S-trihydroxy-(8β)-prosta-5Z,13E-dien-1-oic-3,3,4,4-d4 acid	$C_{20}H_{30}D_4O_5$	316350	211105-40-7	358.48	
d_4-PGF2α	Prostaglandin F2α-d_4	9α,11α,15S-trihydroxy-prosta-5Z,13E-dien-1-oic-3,3,4,4-d4 acid	$C_{20}H_{30}D_4O_5$	316010	34210-11-2	358.48	
d_{11}-5-iPF2α-VI	(±)5-iPF2α-VI-d_{11}	(±)5,9α,11α-trihydroxy-(8β)-prosta-6E,14Z-dien-1-oic-16,16,17,17,18,18,19,19,20,20,20-d11 acid	$C_{20}H_{23}D_{11}O_5$	10006654	936565-17-2	365.57	
d_{11}-8,12-iso-iPF2α-VI	8,12-iso-iPF2α-VI-d_{11}	(12α)-5,9α,11α-trihydroxy-prosta-6E,14Z-dien-1-oic-16,16,17,17,18,18,19,19,20,20,20-d11 acid	$C_{20}H_{23}D_{11}O_5$	10006878	1616977-85-5	365.6	
d_4-8iso-PGE2	8-iso Prostaglandin E2-d_4	9-oxo-11α,15S-dihydroxy-(8β)-prosta-5Z,13E-dien-1-oic-3,3,4,4-d4 acid	$C_{20}H_{28}D_4O_5$	10011321	34210-10-1	356.5	
d_4-PGE2	Prostaglandin E2-d_4	9-oxo-11α,15S-dihydroxy-prosta-5Z,13E-dien-1-oic-3,3,4,4-d4 acid	$C_{20}H_{28}D_4O_5$	314010	1356347-42-6	361.5	
d_4-PGD2	Prostaglandin D2-d_4	9α,15S-dihydroxy-11-oxo-prosta-5Z,13E-dien-1-oic-3,3,4,4-d4 acid	$C_{20}H_{28}D_4O_5$	312010	211105-29-2	356.5	
d_9-PGE2	Prostaglandin E2-d_9	9-oxo-11α,15S-dihydroxy-prosta-5Z,13E-dien-1-oic-17,17,18,18,19,19,20,20,20-d9 acid	$C_{20}H_{23}D_9O_5$	10581	1356347-42-6	361.5	

Abbr.	Common Name	Systematic name	Molecular formula	Cayman	CAS	Mass	HMDB
d_4-LTB4	Leukotriene B4-d_4	5S,12R-dihydroxy-6Z,8E,10E,14Z-eicosatetraenoic-6,7,14,15-d4 acid	$C_{20}H_{28}D_4O_4$	320110	124629-74-9	340.5	
d_4-12,13-DiHOME	(±)12(13)-DiHOME-d_4	(±)12,13-dihydroxy-9Z-octadecenoic-9,10,12,13-d4 acid	$C_{18}H_{30}D_4O_4$	10009994		318.5	
d_4-9,10-DiHOME	(±)9(10)-DiHOME-d_4	(±)9,10-dihydroxy-12Z-octadecenoic-9,10,12,13-d4 acid	$C_{18}H_{30}D_4O_4$	10009993		318.5	
d_{11}-14,15-DiHETrE	(±)14(15)-DiHET-d_{11}	(±)14,15-dihydroxy-5Z,8Z,11Z-eicosatrienoic-16,16,17,17,18,18,19,19,20,20,20-d11 acid	$C_{20}H_{23}D_{11}O_4$	10008040		349.6	
d_6-20-HETE	20-HETE-d_6	20-hydroxy-5Z,8Z,11Z,14Z-eicosatetraenoic-16,16,17,17,18,18-d6 acid	$C_{20}H_{26}D_6O_3$	390030	2548939-89-3	326.5	

Supplementary Table 2. Calibrant concentrations of oxylipins

Calibration concentrations (pM)	C11	C10	C9	C8	C7	C6	C5	C4	C3	C2	C1
20-hydroxy-PGF2α	29925.0	14962.5	7481.3	3740.6	1870.3	935.2	467.6	233.8	116.9	58.4	29.2
20-hydroxy-PGE2	21300.0	10650.0	5325.0	2662.5	1331.3	665.6	332.8	166.4	83.2	41.6	20.8
2,3dinor-8iso-PGF2α	37500.0	18750.0	9375.0	4687.5	2343.8	1171.9	585.9	293.0	146.5	73.2	36.6
20-carboxy-LTB4	20625.0	10312.5	5156.3	2578.1	1289.1	644.5	322.3	161.1	80.6	40.3	20.1
2,3dinor-11β-PGF2α	37500.0	18750.0	9375.0	4687.5	2343.8	1171.9	585.9	293.0	146.5	73.2	36.6
20-hydroxy-LTB4	20850.0	10425.0	5212.5	2606.3	1303.1	651.6	325.8	162.9	81.4	40.7	20.4
iPF2α-IV	37500.0	18750.0	9375.0	4687.5	2343.8	1171.9	585.9	293.0	146.5	73.2	36.6
8iso-15R-PGF2α	37500.0	18750.0	9375.0	4687.5	2343.8	1171.9	585.9	293.0	146.5	73.2	36.6
8iso-PGF2α	37500.0	18750.0	9375.0	4687.5	2343.8	1171.9	585.9	293.0	146.5	73.2	36.6
11β-PGF2α	29625.0	14812.5	7406.3	3703.1	1851.6	925.8	462.9	231.4	115.7	57.9	28.9
PGF2α	37500.0	18750.0	9375.0	4687.5	2343.8	1171.9	585.9	293.0	146.5	73.2	36.6
PGE3	37500.0	18750.0	9375.0	4687.5	2343.8	1171.9	585.9	293.0	146.5	73.2	36.6
PGD3	37500.0	18750.0	9375.0	4687.5	2343.8	1171.9	585.9	293.0	146.5	73.2	36.6
8iso-PGE2	37500.0	18750.0	9375.0	4687.5	2343.8	1171.9	585.9	293.0	146.5	73.2	36.6
PGE2	37500.0	18750.0	9375.0	4687.5	2343.8	1171.9	585.9	293.0	146.5	73.2	36.6
11β-PGE2	29775.0	14887.5	7443.8	3721.9	1860.9	930.5	465.2	232.6	116.3	58.2	29.1
PGD2	37500.0	18750.0	9375.0	4687.5	2343.8	1171.9	585.9	293.0	146.5	73.2	36.6
5-iPF2α -VI	37500.0	18750.0	9375.0	4687.5	2343.8	1171.9	585.9	293.0	146.5	73.2	36.6
8,12-iPF2α-VI	37500.0	18750.0	9375.0	4687.5	2343.8	1171.9	585.9	293.0	146.5	73.2	36.6
9,12,13-TriHOME	60225.0	30112.5	15056.3	7528.1	3764.1	1882.0	941.0	470.5	235.3	117.6	58.8
9,10,13-TriHOME	60375.0	30187.5	15093.8	7546.9	3773.4	1886.7	943.4	471.7	235.8	117.9	59.0
8iso-13,14dihydro-15keto-PGF2α	37500.0	18750.0	9375.0	4687.5	2343.8	1171.9	585.9	293.0	146.5	73.2	36.6
13,14dihydro-15keto-PGF2α	29625.0	14812.5	7406.3	3703.1	1851.6	925.8	462.9	231.4	115.7	57.9	28.9
13,14dihydro-PGF2α	29475.0	14737.5	7368.8	3684.4	1842.2	921.1	460.5	230.3	115.1	57.6	28.8
13,14dihydro-15keto-PGE2	29775.0	14887.5	7443.8	3721.9	1860.9	930.5	465.2	232.6	116.3	58.2	29.1
13,14dihydro-15keto-PGD2	29775.0	14887.5	7443.8	3721.9	1860.9	930.5	465.2	232.6	116.3	58.2	29.1

Calibration concentrations (pM)	C11	C10	C9	C8	C7	C6	C5	C4	C3	C2	C1
5S,6R-lipoxinA4	20850.0	10425.0	5212.5	2606.3	1303.1	651.6	325.8	162.9	81.4	40.7	20.4
5S,6S-lipoxinA4	20850.0	10425.0	5212.5	2606.3	1303.1	651.6	325.8	162.9	81.4	40.7	20.4
1a,1b-dihomo-PGF2α	27450.0	13725.0	6862.5	3431.3	1715.6	857.8	428.9	214.5	107.2	53.6	26.8
bicyclo-PGE2	31425.0	15712.5	7856.3	3928.1	1964.1	982.0	491.0	245.5	122.8	61.4	30.7
8,15-DiHETE	20925.0	10462.5	5231.3	2615.6	1307.8	653.9	327.0	163.5	81.7	40.9	20.4
10,17-DiHDoHE	21000.0	10500.0	5250.0	2625.0	1312.5	656.3	328.1	164.1	82.0	41.0	20.5
17,18-DiHETE	30000.0	15000.0	7500.0	3750.0	1875.0	937.5	468.8	234.4	117.2	58.6	29.3
14,15-DiHETE	30000.0	15000.0	7500.0	3750.0	1875.0	937.5	468.8	234.4	117.2	58.6	29.3
12,13-DiHOME	41400.0	20700.0	10350.0	5175.0	2587.5	1293.8	646.9	323.4	161.7	80.9	40.4
14,15-DiHETrE	21075.0	10537.5	5268.8	2634.4	1317.2	658.6	329.3	164.6	82.3	41.2	20.6
12-HHTrE	21000.0	10500.0	5250.0	2625.0	1312.5	656.3	328.1	164.1	82.0	41.0	20.5
19,20-DiHDPA	20850.0	10425.0	5212.5	2606.3	1303.1	651.6	325.8	162.9	81.4	40.7	20.4
11,12-DiHETrE	21075.0	10537.5	5268.8	2634.4	1317.2	658.6	329.3	164.6	82.3	41.2	20.6
9-HOTrE	42825.0	21412.5	10706.3	5353.1	2676.6	1338.3	669.1	334.6	167.3	83.6	41.8
8,9-DiHETrE	21000.0	10500.0	5250.0	2625.0	1312.5	656.3	328.1	164.1	82.0	41.0	20.5
18-HEPE	23100.0	11550.0	5775.0	2887.5	1443.8	721.9	360.9	180.5	90.2	45.1	22.6
15-HEPE	21150.0	10575.0	5287.5	2643.8	1321.9	660.9	330.5	165.2	82.6	41.3	20.7
20-HETE	21000.0	10500.0	5250.0	2625.0	1312.5	656.3	328.1	164.1	82.0	41.0	20.5
5,6-DiHETrE	21075.0	10537.5	5268.8	2634.4	1317.2	658.6	329.3	164.6	82.3	41.2	20.6
12-HEPE	21150.0	10575.0	5287.5	2643.8	1321.9	660.9	330.5	165.2	82.6	41.3	20.7
9-HEPE	23100.0	11550.0	5775.0	2887.5	1443.8	721.9	360.9	180.5	90.2	45.1	22.6
13-HODE	42525.0	21262.5	10631.3	5315.6	2657.8	1328.9	664.5	332.2	166.1	83.1	41.5
12,13-EpOME	41100.0	20550.0	10275.0	5137.5	2568.8	1284.4	642.2	321.1	160.5	80.3	40.1
5-HEPE	21150.0	10575.0	5287.5	2643.8	1321.9	660.9	330.5	165.2	82.6	41.3	20.7
9-HODE	42525.0	21262.5	10631.3	5315.6	2657.8	1328.9	664.5	332.2	166.1	83.1	41.5
9,10-EpOME	41100.0	20550.0	10275.0	5137.5	2568.8	1284.4	642.2	321.1	160.5	80.3	40.1

Calibration concentrations (pM)	C11	C10	C9	C8	C7	C6	C5	C4	C3	C2	C1
17-HDoHE	21375.0	10687.5	5343.8	2671.9	1335.9	668.0	334.0	167.0	83.5	41.7	20.9
20-HDoHE	21375.0	10687.5	5343.8	2671.9	1335.9	668.0	334.0	167.0	83.5	41.7	20.9
16-HDoHE	21375.0	10687.5	5343.8	2671.9	1335.9	668.0	334.0	167.0	83.5	41.7	20.9
16,17-EpDPE	30525.0	15262.5	7631.3	3815.6	1907.8	953.9	477.0	238.5	119.2	59.6	29.8
9-HETE	21000.0	10500.0	5250.0	2625.0	1312.5	656.3	328.1	164.1	82.0	41.0	20.5
11,12-EpETrE	21000.0	10500.0	5250.0	2625.0	1312.5	656.3	328.1	164.1	82.0	41.0	20.5
14-HDoHE	21375.0	10687.5	5343.8	2671.9	1335.9	668.0	334.0	167.0	83.5	41.7	20.9
10-HDoHE	21375.0	10687.5	5343.8	2671.9	1335.9	668.0	334.0	167.0	83.5	41.7	20.9
12-HETE	21000.0	10500.0	5250.0	2625.0	1312.5	656.3	328.1	164.1	82.0	41.0	20.5
11-HDoHE	21375.0	10687.5	5343.8	2671.9	1335.9	668.0	334.0	167.0	83.5	41.7	20.9
8-HDoHE	21375.0	10687.5	5343.8	2671.9	1335.9	668.0	334.0	167.0	83.5	41.7	20.9
8-HETrE	22800.0	11400.0	5700.0	2850.0	1425.0	712.5	356.3	178.1	89.1	44.5	22.3
5-HETrE	22800.0	11400.0	5700.0	2850.0	1425.0	712.5	356.3	178.1	89.1	44.5	22.3
5S,14R-lipoxinB4	20850.0	10425.0	5212.5	2606.3	1303.1	651.6	325.8	162.9	81.4	40.7	20.4

Supplementary Table 3. Mass spectrometer parameters in the developed micro-LC-MS/MS method

Compound Name	Q1 mass	Q3 mass	Dwell time	EP	CE	CXP	Q0D	Retention time (min)
20-hydroxy-PGF2α	369.2	325.2	200.00	-12	-28	-15	-25	10.02
20-hydroxy-PGE2	367.2	287.2	200.00	-11	-22	-14	-25	10.16
2,3dinor-8iso-PGF2α	325.1	237.2	200.00	-9	-16	-15	-25	13.67
2,3dinor-11β-PGF2α	325	145.2	200.00	-9	-23	-13	-25	14.77
20-carboxy-LTB4	365.2	347.2	200.00	-10	-23	-16	-25	16.35
20-hydroxy-LTB4	351.2	195.2	200.00	-7	-23	-10	-25	17.17
iPF2α-IV	353.3	127.1	200.00	-11	-29	-14	-25	18.55
d_4-8iso-PGF2α-ISTD	357.3	197.15	200.00	-10	-33	-13	-25	19.46
PGE3; PGD3	349.2	269.2	200.00	-10	-21	-12	-25	20.0
d_{11}-5-iPF2α-VI-ISTD	364.2	115.05	169.25	-10	-30	-13	-25	20.45
5-iPFα-VI	353.2	115.05	162.12	-10	-28	-10	-25	20.8
8iso-15R-PGF2α;8iso-PGF2α;11β-PGF2α;PGF2α	353.1	193.1	200.00	-10	-33	-10	-25	21.0
9,12,13-TriHOME	329.2	211.1	170.46	-9	-29	-10	-50	22.03
9,10,13-TriHOME	329.2	171.1	127.11	-10	-33	-11	-50	22.43
d_4-PGF2α-ISTD	357.3	197.15	125.20	-10	-33	-13	-25	22.5
8iso-13,14dihydro-15keto-PGF2α	353.3	183.1	135.84	-8	-32	-9	-25	22.88
d_9-PGE2-ISTD	360.3	280.25	152.01	-10	-21	-13	-25	23.13
d_4-8iso-PGE2-ISTD;d_4-PGE2-ISTD;d_4-PGD2-ISTD	355.3	275.25	183.42	-10	-21	-13	-25	23.2
8iso-PGE2; PGE2; 11β-PGE2; PGD2	351.1	271.15	165.78	-8	-23	-14	-25	23.5
5S,14R-lipoxinB4	351.2	221.2	200.00	-14	-20	-10	-35	24.05
13,14dihydro-PGF2α	355.2	311.3	189.05	-13	-31	-17	-25	24.51
d_{11}-8,12-iso-iPF2α-VI-ISTD	364.21	115.05	148.55	-10	-30	-13	-25	25.1
8,12-iso-iPF2α-VI	353.21	115.05	144.80	-7	-25	-13	-25	25.2
5S,6S-LipoxinA4	351.21	115.2	153.12	-13	-20	-13	-35	25.41
13,14dihydro-15keto-PGE2	351.2	175.1	160.38	-13	-30	-8	-25	25.52
13,14dihydro-15keto-PGF2α	353.31	183.1	161.00	-11	-35	-16	-25	25.53
5S,6R-LipoxinA4	351.2	115.2	200.00	-14	-35	-10	-35	25.91
1a-1b-dihomo-PGF2α	381.1	337.45	200.00	-13	-29	-13	-25	26.43
13,14dihydro-15keto-PGD2	351.21	175.1	200.00	-11	-27	-13	-25	26.59
8,15-DiHETE	335.2	235.1	200.00	-13	-12	-11	-50	28.47
bicyclo-PGE2	333.2	113.15	200.00	-13	-33	-13	-25	28.75
17,18-DiHETE	335.2	247.1	185.52	-8	-24	-11	-50	28.98
10,17-DiHDoHE	359.2	153.1	176.57	-13	-24	-14	-50	29.06
d_4-LTB4-ISTD	339.5	197.1	171.63	-10	-20	-13	-50	29.18

14,15-DiHETE	335.2	207.1	161.35	-7	-22	-10	-50	29.57
d_4-12,13-DiHOME-ISTD	317.2	185.1	142.71	-10	-30	-13	-50	29.95
12,13-DiHOME	313.2	183.1	144.99	-11	-30	-11	-50	30.04
d_4-9,10-DiHOME-ISTD	317.2	203.1	151.84	-10	-30	-13	-50	30.38
d_{11}-14,15-DiHETrE-ISTD	348.2	207.1	176.19	-10	-24	-13	-50	31.2
14,15-DiHETrE	337.2	207.1	178.48	-9	-24	-9	-50	31.3
12-HHTrE	279.2	179.1	189.13	-11	-18	-10	-50	31.4
19,20-DiHDPa	361.2	273.2	200.00	-10	-21	-13	-50	31.5
11,12-DiHETrE	337.2	167.3	200.00	-7	-24	-14	-50	32.2
9-HOTrE	293.2	171.2	162.00	-9	-22	-10	-50	32.64
8,9-DiHETrE	337.2	127.2	152.47	-10	-27	-14	-50	32.67
18-HEPE	317.2	299.2	98.84	-11	-18	-14	-50	32.92
5,6-DiHETrE	337.2	145.15	59.84	-8	-24	-13	-50	33.16
d_6-20-HETE-ISTD	325.2	279.2	55.36	-10	-21	-13	-50	33.24
15-HEPE	317.2	219.2	54.70	-8	-18	-11	-50	33.26
20-HETE	319.2	289.2	53.90	-8	-24	-13	-50	33.28
12-HEPE	317.2	179.1	48.05	-9	-18	-14	-50	33.45
9-HEPE	317.2	167.25	46.42	-13	-18	-14	-50	33.51
5-HEPE	317.2	115.2	43.36	-8	-12	-13	-50	33.64
d_4-9-HODE-ISTD	299.2	172.1	40.81	-10	-27	-13	-50	33.74
9-HODE	295.21	171.1	40.81	-8	-15	-15	-50	33.74
13-HODE	295.2	195.2	40.81	-10	-15	-14	-50	33.75
20-HDoHE	343.21	299.2	40.25	-15	-18	-16	-50	33.85
16-HDoHE	343.2	233.2	39.63	-12	-18	-10	-45	34.02
16,17-EpDPE	343.21	233.2	39.63	-10	-15	-11	-50	34.02
11,12-EpETrE	319.22	167.1	40.61	-10	-18	-15	-45	34.12
9-HETE	319.21	167.1	40.91	-9	-10	-15	-50	34.13
10-HDoHE	343.21	153.1	42.16	-14	-21	-15	-40	34.17
14-HDoHE	343.2	205.1	42.16	-7	-18	-15	-50	34.18
d_8-12-HETE-ISTD	327.2	184.1	43.76	-10	-21	-13	-50	34.21
12-HETE	319.2	179.2	47.17	-12	-10	-14	-50	34.28
11-HDoHE	343.2	121.1	47.17	-11	-18	-14	-45	34.28
8-HDoHE	343.2	189.1	55.57	-14	-15	-15	-45	34.4
8-HETrE	321.2	303.2	55.57	-12	-18	-16	-40	34.4
17-HDoHE	343.2	281.2	103.43	-13	-16	-13	-50	34.5
5-HETrE	321.21	303.2	79.86	-7	-18	-15	-50	34.55
12,13-EpOME	295.21	195.2	167.46	-7	-21	-13	-45	34.9
9,10-EpOME	295.22	171.1	200.00	-8	-21	-9	-50	34.98

Supplementary Table 4. UHPLC gradients used in the comparison experiment

Mobile phase A: H_2O with 0.1 % acetic acid; mobile phase B: 90 % ACN/10 % MeOH with 0.1 % acetic acid; mobile phase C: IPA with 0.1 % acetic acid with pH ranges between 3.2 and 3.5

Time [min]	Flow [mL/min]	B.Conc [%]	C.Conc [%]
0.75	0.70	20.0	1.0
0.95	0.70	26.0	1.0
6.00	0.70	34.0	1.0
8.00	0.70	40.0	1.0
10.00	0.70	54.0	1.0
11.00	0.70	55.0	1.0
12.00	0.70	56.0	3.0
13.00	0.70	78.0	6.0
14.00	0.70	85.0	15.0
14.50	0.70	85.0	15.0
14.80	0.70	20.0	1.0
16.00	0.70	20.0	1.0

Supplementary Table 5. Comparison of LODs and LOQs of micro flow-LC-MS/MS and UHPLC-MS/MS methods

Compounds	LOD (pM)		Fold Change	LOQ (pM)	
	micro flow-LC-MS/MS	UHPLC-MS/MS		micro flow-LC-MS/MS	UHPLC-MS/MS
13-HODE	59.0	-	-	196.6	-
8,12-iPF2α-IV	23.0	-	-	76.5	-
13,14dihydro-15keto-PGE2	0.3	-	-	0.9	-
19,20-DiHDPA	0.1	19.9	180.7	0.4	66.3
5S,6S-LipoxinA4	0.1	16.9	170.2	0.3	56.2
iPF2α-IV	0.2	28.0	114.4	0.8	93.2
2,3dinor-8iso-PGF2α	0.3	34.6	102.3	1.1	115.4
PGE3	0.1	7.4	71.4	0.3	24.7
8iso-PGE2	0.1	4.9	56.9	0.3	16.3
11,12-DiHETrE	0.1	5.6	50.8	0.4	18.6
PGF2α	0.2	11.6	48.4	0.8	38.7
15-HEPE	0.4	13.7	31.2	1.5	45.8
2,3dinor-11β-PGF2α	1.2	29.4	23.8	4.1	98.1
8iso-13,14dihydro-15keto-PGF2α	1.1	24.7	23.0	3.6	82.5
11β-PGE2	0.3	6.1	21.4	0.9	20.2
13,14dihydro-15keto-PGD2	0.3	6.7	21.1	1.1	22.2
20-hydroxy-LTB4	0.8	16.1	20.8	2.6	53.8
20-carboxy-LTB4	1.3	23.5	18.6	4.2	78.4
8,9-DiHETrE	0.5	8.5	18.0	1.6	28.2
5S,6R-lipoxinA4	1.0	18.1	18.0	3.4	60.4
17,18-DiHETE	2.4	42.7	17.7	8.0	142.4
8iso-PGF2α	2.1	31.3	15.3	6.8	104.3
12-HEPE	0.4	6.1	13.9	1.5	20.3
9,10-EpOME	2.2	28.5	13.0	7.3	94.9

9,12,13-TriHOME	6.6	69.1	10.5	22.0	230.5
14,15-DiHETE	0.7	6.8	10.0	2.3	22.5
16,17-EpDPE	5.1	50.1	9.9	16.8	167.1
20-hydroxy-PGE2	0.3	2.5	8.9	1.0	8.5
18-HEPE	3.0	18.7	6.3	9.9	62.4
12,13-DiHOME	2.3	14.2	6.2	7.6	47.2
5,6-DiHETrE	2.2	13.3	6.0	7.4	44.3
11β-PGF2α	1.1	6.6	5.8	3.8	22.0
PGE2	0.9	4.9	5.6	2.9	16.2
8-HETrE	4.4	21.2	4.9	14.5	70.5
PGD2	0.4	1.8	4.8	1.3	6.1
PGD3	0.6	2.5	4.6	1.8	8.4
1a,1b-dihomo-PGF2α	0.6	2.5	4.0	2.1	8.4
10,17-DiHDoHE	4.7	17.4	3.7	15.8	57.9
8iso-15R-PGF2α	0.8	3.0	3.6	2.8	9.9
9-HEPE	3.9	13.5	3.5	12.9	45.0
9-HOTrE	2.6	9.1	3.4	8.8	30.4
14,15-DiHETrE	0.9	2.9	3.3	3.0	9.8
8,15-DiHETE	6.1	17.9	2.9	20.5	59.8
bicyclo-PGE2	0.9	2.6	2.9	3.0	8.8
13,14dihydro-PGF2α	3.5	9.7	2.8	11.7	32.4
12-HHTrE	4.4	12.2	2.8	14.7	40.7
11,12-EpETrE	0.6	1.5	2.7	1.8	5.0
20-hydroxy-PGF2α	1.9	5.0	2.7	6.2	16.6
5-iPF2α-VI	2.5	6.6	2.6	8.3	22.0
12,13-EpOME	4.3	10.6	2.5	14.4	35.3
5-HETrE	4.7	10.4	2.2	15.6	34.7
9,10,13-TriHOME	4.6	9.5	2.1	15.4	31.8
14-HDoHE	7.1	10.4	1.5	23.6	34.5
20-HETE	8.8	12.5	1.4	29.3	41.8
13,14dihydro-15keto-PGF2α	2.5	2.4	1.0	8.5	8.1
5S,14R-lipoxinB4	11.6	11.0	0.9	38.6	36.7
9-HETE	8.3	7.0	0.8	27.8	23.3
11-HDoHE	8.8	6.8	0.8	29.2	22.8
10-HDoHE	12.8	9.4	0.7	42.6	31.3
9-HODE	27.7	17.8	0.6	92.3	59.3
16-HDoHE	3.4	1.9	0.5	11.5	6.2
5-HEPE	5.7	2.3	0.4	19.1	7.7
12-HETE	21.9	6.3	0.3	72.9	21.0
17-HDoHE	47.3	6.4	0.1	157.6	21.5
20-HDoHE	91.9	10.3	0.1	306.2	34.5
8-HDoHE	76.4	4.7	0.1	254.6	15.8

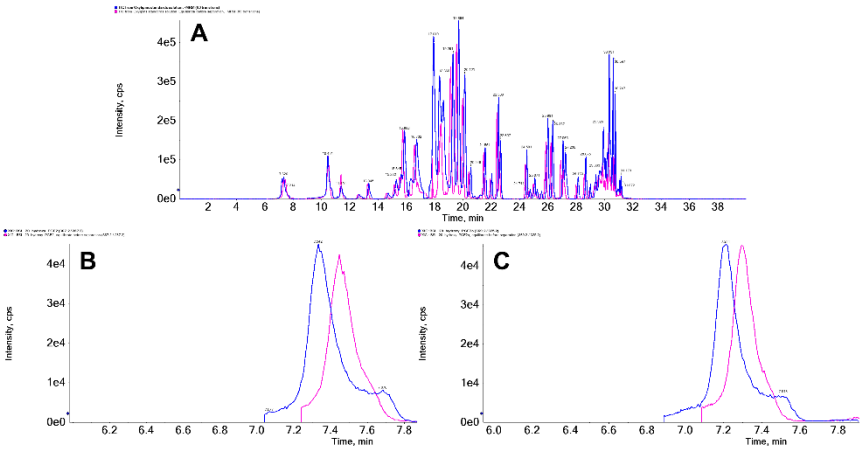

Supplementary Figure 1. Effect of equilibration time on early eluted compounds. A. Total ion chromatogram from injections of oxylipins standard solution; B. Extracted SRM chromatograms of 20-hydroxy-PGE2; C. Extracted SRM chromatograms of 20-hydroxy-PGF2α. Blue line represents the analysis with 1.5-min initial gradient, red line represents analysis with 5.5-min initial gradient.